Showa Univ J Med Sci 33(3), 88-95, September 2021

Original Paper

# Computational fluid dynamics analysis in patients with nasal disease

Emina Masuda*[1], Akiko Ishizaki[1], Kojiro Hirano[2], Tomonori Iwasaki[3], Takehiko Sambe[4], Chiaki Sawaguchi[5] and Shouji Hironaka[1]

Received: 26 February 2021 / Accepted: 15 March 2021

**Abstract**

Computational fluid dynamics (CFD) analysis is useful for quantitative assessment in patients with upper airway obstructions. We compared CFD analysis with rhinomanometry (RM) and acoustic rhinometry (AR). Twenty patients with nasal and paranasal diseases who required computed tomography assessment underwent RM and AR. We measured the pressure and velocity at four parts of the upper airway using CFD analysis. Then we evaluated the correlation among CFD analysis, RM, and AR. CFD analysis detected obstruction sites in the nasal airway and pharynx in 14 and 2 patients, respectively. High negative pressure accompanied the nasal obstruction, even behind the nasal cavity. Nasal airway pressure measured using CFD analysis strongly correlated with nasal resistance in RM (Spearman correlation coefficient = 0.853). CFD analysis's sensitivity and specificity to detect the obstruction were 84.6% and 57.1%, respectively (compared to those of RM) and 83.3% and 50.0%, respectively (compared to those of AR). The CFD analysis's ability to detect obstruction was comparable to that of RM and AR; therefore, it may help evaluate the upper airways in patients with nasal and paranasal diseases. We found impaired nasal ventilation also affected other parts of the upper airway. Further studies with a larger sample size are required to validate the use of CFD analysis for assessing the degree of upper airway ventilation disorders.

**Key words**: acoustic rhinometry, allergic rhinitis, computational fluid dynamics, rhinomanometry, sinusitis

## Introduction

Computational fluid dynamics (CFD) analysis evaluates upper airway disorders and evaluates both the morphology and airway ventilation status in contrast to computed tomography (CT) that can only evaluate the morphology[1]. Many studies have described the use of CFD analysis for examining patients with obstructive sleep apnea syndrome (OSAS) and skeletal malocclusion; however, few reports have performed a quantitative evaluation of the pressure and velocity[2–5]. Studies show CFD analysis has been used to examine the nasal airway for nasal septal perforation[6, 7] and the effect of surgical effects on simulation[8, 9], however, all these studies enrolled healthy adults. One study investigated patients with deviated nasal septum; however, patients with non-structural causes of nasal airway obstruction, such as rhinitis, sinusitis, and tumoral/autoimmune processes, were excluded[10], CFD was used for the only nasal airway in this study. Wakayama *et al*. included the results of CFD analysis in patients with nasal and paranasal diseases with nasal obstruction[11]. They assessed pressure loss coefficients and velocities using CFD analysis in 16 patients with OSAS. They determined nasal obstruction based on the presence of nasal diseases and paranasal diseases and rhinomanometry (RM) results. Nine of the

* Corresponding author
✉ Emina Masuda
eminamasuda0210@gmail.com

[1] Department of Special Needs Dentistry, Division of Hygiene and Oral Health, Showa University School of Dentistry, 1-5-8 Hatanodai, Shinagawa-ku, Tokyo 142-8555, Japan.
[2] Department of Otorhinolaryngology, Showa University School of Medicine.
[3] Department of Pediatric Dentistry, Tokushima University Graduate School of Biomedical Sciences.
[4] Department of Pharmacology, Showa University School of Medicine.
[5] Radiology Showa University Hospital.

16 patients had a nasal obstruction, and Wakayama *et al*. compared CFD analysis results to those of the control group (no nasal obstruction) in seven patients. The primary differences between the present study and the previous study were as follows: the previous study focused only on nasal analysis, CT was performed using continuous positive airway pressure (CPAP), and all participants had OSAS.

To our knowledge, CFD analysis has not been previously performed for the upper airway of patients with nasal paranasal diseases and nasal obstruction. Further, as per our literature review, no studies have evaluated the obstruction site in the upper airway using CFD analysis in patients with nasal and paranasal diseases. Nasal obstruction is one of several upper airway ventilation disorders and a primary symptom of nasal and paranasal diseases. Therefore, we believe that it is crucial to examine the entire upper airway rather than only the nasal airway. We evaluated the ability of CFD analysis to assess upper airway ventilation in patients with clinically diagnosed nasal and paranasal diseases. Moreover, we compared the CFD analysis results with RM and acoustic rhinometry (AR), an existing assessment for nasal obstruction[12, 13]. To our knowledge, this is the first study to quantitatively evaluate the ventilation status of any site of the upper airway in patients with nasal and paranasal diseases using CFD analysis.

## Materials and methods

*1. Participants*

From January 1, 2020, to April 7, 2020, patients with nasal and paranasal diseases who underwent CT and visited the Department of Otolaryngology, Showa University Hospital, were invited to participate in our study. Twenty patients aged $>$ 20 y who were prescribed CT and RM by the attending physician were recruited after they provided informed consent for study participation. The Institutional Ethical Committee of the Showa University School of Medicine, Japan, approved the experimental protocols (Permission Number: 3003).

*2. Assessments*

All 20 participants underwent CT (SOMATOM Force, SOMATOM Sensation 64, SOMATOM Definition AS+; Siemens, Germany), RM, (NR6 EXECUTIVE; GM, UK), and AR (NR6 EXECUTIVE; GM, UK). CT was performed on 0.75 mm slices from the nasal and paranasal to the oropharyngeal airway, including the glottal. RM and AR were performed on the same day as the CT without leaving the time. To match the posture at the time of the CT, we performed RM and AR, with the patient in the supine position[14–16], three times per patient, and recorded the average value. Nasal airway resistance (NAR) was defined as abnormal when it exceeded 0.25 Pa/cm$^3$/s, the normal Japanese value, as per the Japanese RM guideline[17]. AR was defined as abnormal when it deviated from the range of the minimum cross-sectional area (MCA) 0.75 $\pm$ 0.26 cm$^2$, the Japanese reference value from the Japanese AR guideline[18].

*3. Functional evaluation of the upper airway*

We manually generated the three-dimensional (3D) upper airway from the CT data using volume-rendering software (INTAGE Volume Editor; Cybernet Systems, Tokyo, Japan)[19, 20]. The airway was segmented primarily based on the image intensity, with the threshold set midway between the soft tissue and clear airway values. Subsequently, using mesh-morphing software (DEP MeshWorks/Morpher; IDAJ, Kobe, Japan), the 3D-model was smoothed without compromising the patient-specific pattern of the airway shapes. We exported the models to CFD software (PHOENICS; CHAM Japan, Tokyo, Japan) as stereolithography files and set up the 3D model under the following conditions: the wall surface was nonslip, and the model was rigid.

The upper airway models' CFD analysis used a volume of airflow at a volumetric flow rate of 500 cm$^3$/s, assuming a non-slippery wall surface. We performed the simulations to estimate the airflow pressure; air flowed horizontally from the choana and was exhaled through both the external nostrils. Simulations were repeated 1,000 times to generate average values. We conducted an inspiration simulation of the upper airway (air flowing in the nares at a volume of airflow at a volumetric flow rate of 500 cm$^3$/s)[21]. We estimated the pressures and velocity in different parts of the upper airway (nasal airway, nasopharyngeal airway [NA], retropalatal airway [RA], and oropharyngeal airway [OA]) (Figure 1). The measurement range of the nasal airway was the range surrounded by the PNS plane and PL plane. Negative values indicated inspiratory pressures in each part of the upper airway. We defined airway obstruction as 0.25 Pa/cm$^3$/s, corresponding to a resistance level equivalent to about −120 Pa as per our flow quantity settings (volumetric flow rate of 500 cm$^3$/s)[2]. Thus, we concluded that obstruction occurs when negative pressure exceeds −120 Pa. Previous studies have also suggested that a velocity

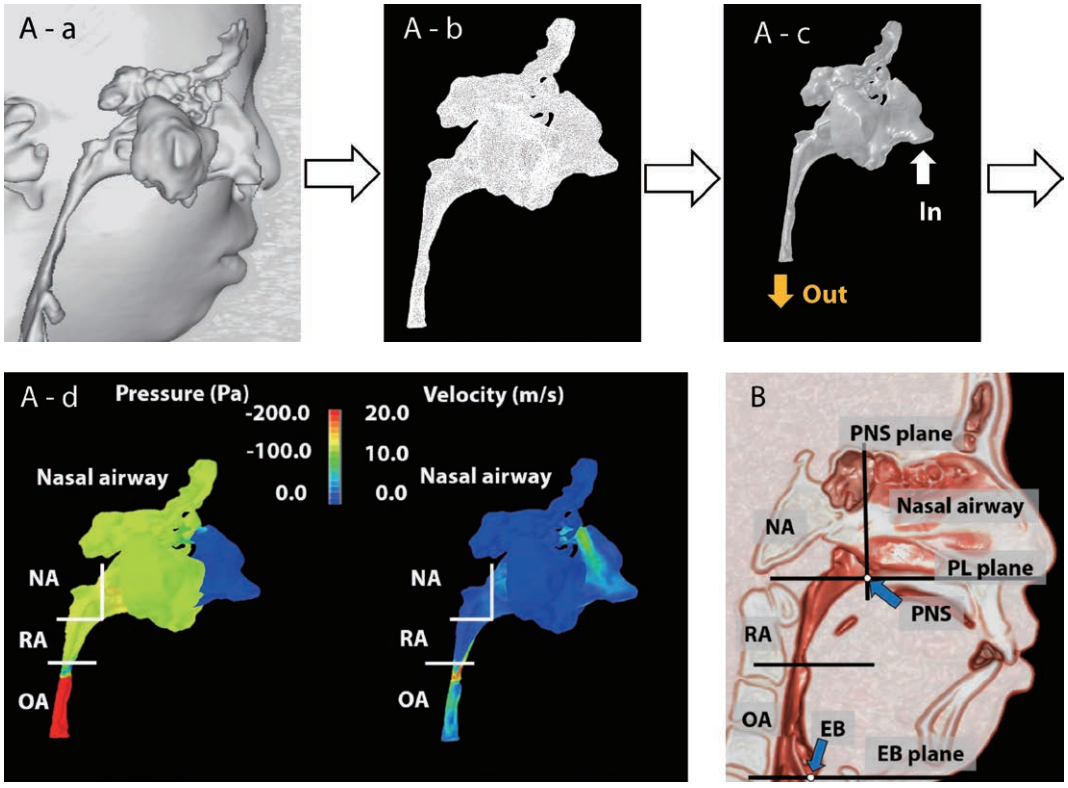


Fig. 1. (A–a) 3D model of maxillofacial included upper airway built using the computed tomography (CT) data, (A–b) volume rendering and smoothing after that extracted the upper airway image from the 3D model, (A–c) fluid-mechanical simulation at intake conditions, (A–d) evaluation of the upper airway ventilation condition using pressure and velocity, (B) landmarks and planes for the axial airway section. PNS = posterior nasal spine, PNS plane = the plane perpendicular to the hard palate passing through the PNS, PL plane = the plane parallel to the hard palate passing through the PNS, EB = base of the epiglottis, EB plane = the plane parallel to the PL plane passing through the EB, Nasal airway = The part front of the nasal cavity surrounded by PNS and PL planes, NA = The part after the nasal cavity surrounded by the PNS plane and the PL plane, RA = Pharynx from the PL plane to the tip of the soft palate, OA = Pharynx from the tip of the soft palate to the EB plane.

of ≥ 12 m/s signifies an obstruction[2, 21–23]. Therefore, in the present study, obstruction sites had a pressure of ≤ −120 Pa and a velocity of ≥ 12 m/s. The maximum velocity and negative pressure were defined as the largest values measured in the upper airway.

*4. Statistical analyses*

We evaluated the data using IBM SPSS Statistics, version 23 (SPSS Company, Chicago, IL, USA). Spearman's correlation was used to evaluate the correlations among RM, AR, and CFD. A p-value $< 0.05$ was statistically significant. Moreover, comparisons between RM and AR and CFD were based on sensitivity and specificity.

## Results

*1. Participant characteristics and assessment*

The final sample comprised 12 men and eight women, with an average age of 47.45 ± 16.95 y. We found that 70.0% of the study subjects had allergic rhinitis, and 55.0% had sinusitis (Table 1). The participants' bilateral NAR was higher than the normal Japanese value in 13 of the 20 subjects[17]. Eleven of the subjects had an obstruction site in their nasal airway, as measured using CFD analysis. The MCA deviated from the Japanese reference value in 12 of the 20 subjects[18]. Ten of the subjects had an obstruction site in their nasal airway, as measured using CFD analysis. In the CFD analysis, the nasal airway's negative pressure was the lowest at 143.7 ± 34.3 Pa, gradually rising as it went downstream of the

Table 1. Clinical characteristics of patients with nasal diseases

| | Mean (± S. D) | Mean of men (± S. D) | Mean of female (± S. D) |
|---|---|---|---|
| Age (y) | 47.45 (16.95) | 45.59 (16.56) | 51.79 (15.94) |
| Sex (M : F) | 12 : 8 | - | - |
| Height (cm) | 167.23 (7.14) | 171.58 (3.75) | 160.69 (5.37) |
| Body weight (kg) | 67.08 (16.04) | 75.17 (14.54) | 54.94 (6.97) |
| Percentile BMI (% ile) | 23.84 (4.79) | 25.56 (5.09) | 21.25 (2.14) |
| | n (%) | n = 12 | n = 8 |
| Allergic Rhinitis | 15 (75.0) | | |
| Sinusitis | 11 (55.0) | | |
| Deviated nasal septum | 4 (20.0) | | |
| | n = 20 | | |

Table 2. Assessment of the upper airway using RM, AR, and CFD analysis

| | | Mean (± S. D) |
|---|---|---|
| RM/AR | | |
| NAR (Pa/cm$^3$/s) | | 0.289 (0.064) |
| MCA (cm$^2$) | | 1.098 (0.411) |
| LNV (cm$^3$) | | 13.160 (6.172) |
| CFD | | |
| Pressure | Nasal airway (Pa) | −143.7 (34.3) |
| | NA (Pa) | −149.4 (31.1) |
| | RA (Pa) | −177.8 (60.9) |
| | OA (Pa) | −219.5 (163.6) |
| | Max (Pa) | −219.5 (163.6) |
| Velocity | Nasal airway (m/s) | 15.4 (3.6) |
| | NA (m/s) | 2.9 (1.3) |
| | RA (m/s) | 7.7 (6.1) |
| | OA (m/s) | 3.2 (1.8) |
| | Max (m/s) | 16.3 (4.3) |
| | | n = 20 |

Rhinomanometry = RM, AR = Acoustic rhinometry, CFD = computational fluid dynamics, NAR = nasal airway resistance, MCA = minimal cross-sectional area, LNV = lateral nasal volume 0-5 cm, NA = nasopharyngeal airway, RA = retropalatal airway, OA = oropharyngeal airway.

upper airway, and the maximum value was 219.5 ± 163.6 Pa in the OA. The nasal airway was highest at 15.4 ± 3.6 m/s, and RA was the second-highest at 7.7 ± 6.1 m/s (Table 2).

*2. Pressure and velocity*

Table 3 shows the obstruction site evaluation results; 14 of the 20 subjects had an obstruction site in their nasal airway. Further, two of the subjects had an obstruction site in their RA, while four did not have an obstruction site. Figure 2 demonstrates the evaluation of the upper airway ventilation condition using CFD analysis. Patient 20 had no obstruction site, and patient 1 had an obstruction site in the nasal airway. In the case of patient 20, we simulated a low velocity and low negative pressure. For patient 1, we simulated a high velocity and a high negative pressure in the nasal airway. Large negative pressures persisted at the downstream sites.

*3. Correlation of assessment*

Table 4 shows the correlation results of each assessment. CFD analysis showed a high correlation between nasal airway pressure and NAR (R=0.853); however, there was no correlation between the nasal airway velocity and NAR (R=0.403). Similarly, a correlation was observed between the pressure of NA and NAR (R=0.737). Also, there was a correlation between the nasal airway pressure and NA pressure (R=0.874), between the NA pressure and the RA pressure (R=0.686), and between the RA pressure and the OA pressure (R=0.818). Compared to RM, the CFD sensitivity was 84.6%, and its specificity was 57.1%. The CFD sensitivity, compared to AR, was 83.3%, and its specificity was 50.0%.

## Discussion

This study quantitatively evaluated any upper airway site's ventilatory conditions in patients with nasal and paranasal diseases using CFD analysis. The nasal airway pressure measured using CFD analysis strongly correlated with the NAR in RM. In 2020,

Table 3. Pressure and velocity determined using CFD in the patients with nasal diseases

| Case No. | Nasal airway | NA | RA | OA | Obstruction site | Nasal diseases |
|---|---|---|---|---|---|---|
| 1 | * † | † | † | † | Nasal airway | Allergic Rhinitis, Deviated nasal septum |
| 2 | * † | † | † | † | Nasal airway | Allergic Rhinitis |
| 3 | * † | † | † | † | Nasal airway | Allergic Rhinitis |
| 4 | * † | † | * † | † | Nasal airway | Sinusitis, Deviated nasal septum |
| 5 | * † | † | † | † | Nasal airway | Allergic Rhinitis, Sinusitis |
| 6 | * † | † | † | † | Nasal airway | Sinusitis |
| 7 | * † | † | † | † | Nasal airway | Allergic Rhinitis |
| 8 | * † | † | † | † | Nasal airway | Allergic Rhinitis, Sinusitis |
| 9 | * † | † | † | † | Nasal airway | Allergic Rhinitis, Sinusitis |
| 10 | * † | † | † | † | Nasal airway | Allergic Rhinitis |
| 11 | * † | † | † | † | Nasal airway | Sinusitis |
| 12 | * | † | * † | † | RA | Sinusitis |
| 13 | * | | * † | † | RA | Allergic Rhinitis |
| 14 | † | † | † | † | Nothing | Allergic Rhinitis |
| 15 | | † | † | † | Nothing | Allergic Rhinitis, Sinusitis, Deviated nasal septum |
| 16 | * | † | † | † | Nothing | Sinusitis |
| 17 | * | | † | † | Nothing | Allergic Rhinitis, Sinusitis, Deviated nasal septum |
| 18 | * | | | † | Nothing | Allergic Rhinitis |
| 19 | * | | | | Nothing | Allergic Rhinitis |
| 20 | | | | | Nothing | Allergic Rhinitis, Sinusitis |

*The velocity is above 12 m/s. † The pressures are less than −120 pa. NA = nasopharyngeal airway, OA = oropharyngeal airway, RA = retropalatal airway

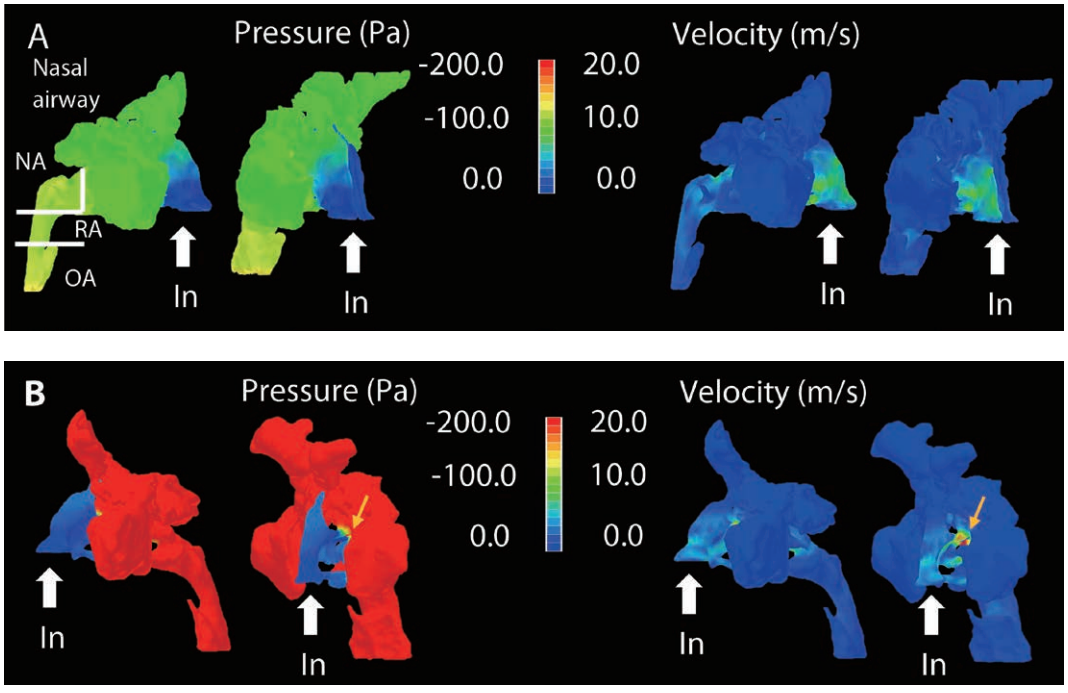


Fig. 2. Evaluation of the upper airway ventilation condition. (A) CFD results in case 20. No obstruction site. (B) CFD results in case 1. The obstruction site is the nasal airway. The right nasal cavity is completely blocked, and the left nasal cavity has advanced nasal ventilation disorder. Both pressure and velocity are high at the site of the yellow arrow.

Yanagisawa *et al*. reported the CFD results in 10 healthy children and 10 pediatric patients with OSAS[2]. The results suggested a negative pressure greater than that calculated from the flow volume and resistance setting, and a velocity of > 12 m/s is reasonable for demarcating the obstruction site. Demarcation was same performed in the present study. Most patients in whom the nasal airway was the obstruction site on CFD analysis also showed abnormality on RM and AR. Compared to that of RM and AR, the sensitivity of CFD analysis shows that CFD analysis has the same evaluation capability as RM and AR. Thus, the figures and the obstruction site derived using the CFD analysis were reasonable.

In this study, the nasal airway was the obstruction site in 14 of the 20 patients. Moreover, many patients with nasal and paranasal diseases and nasal obstruction also had obstruction sites in the nasal airway in the simulation. Also, previous studies have shown that the resistance in the anterior part of the nasal airway causes nasal obstruction. This is consistent with the finding that most study subjects had an obstruction in the nasal airway, the measurement site in front of the nasal airway. Also, if the nasal airway had high negative pressure, high negative pressure was maintained in NA, RA, and OA downstream of the nasal airway. The pressure of the upstream part of the upper airway was highly correlated with the immediately downstream site and negative pressure tended to rise downstream. Thus, the obstruction site may also affect the surrounding site. Furthermore, we believe that a high negative pressure occurred in the upper airway when there was an obstruction site in the nasal airway, possibly reducing the upper airway's ventilatory conditions. The Sterling resistor model supports this result. This model predicts that a further obstruction upstream (nasal cavity) will generate a suction force (negative intraluminal pressure) downstream (oropharynx), resulting in an oropharyngeal collapse in predisposed individuals[24]. The results of the CFD analysis in this study strongly suggested a Sterling resistor model. Therefore, we believe that impaired nasal ventilation also affects other parts of the upper airway[25-28]. Wakayama *et al*. reported higher nasal pressure loss coefficients and faster velocities in patients with nasal obstruction[11]. When the flow rate is constant, a large pressure loss coefficient requires a large pressure. This is consistent with the present finding, wherein CFD results show that the presence of an obstruction site in the nasal airway causes a high velocity in the nasal airway and requires a large pressure. The nasal airway pressure measured using CFD analysis strongly correlated with the NAR determined using RM; thus,

Table 4. Correlations among RM, AR, and CFD

| | | Rhinomanometry, AR | | | CFD pressures (Pa) | | | | CFD velocity (m/s) | | | |
|---|---|---|---|---|---|---|---|---|---|---|---|---|
| | | NAR | MCA | LNV | Nasal airway | NA | RA | OA | Nasal airway | NA | RA | OA |
| Rhinomanometry, AR | NAR | - | −.095 | −.158 | .853** | .737** | .450* | .149 | .403 | .028 | −.252 | −.242 |
| | MCA | | - | .663** | −.108 | −.078 | −.319 | −.340 | .021 | .292 | −.022 | .322 |
| | LNV | | | - | −.183 | −.077 | −.056 | −.008 | −.202 | .397 | .241 | .469* |
| CFD pressure (Pa) | Nasal airway | | | | - | .874** | .498* | .131 | .379 | −.182 | −.296 | −.340 |
| | NA | | | | | - | .686** | .332 | .217 | −.082 | −.193 | −.252 |
| | RA | | | | | | - | .818** | .191 | −.056 | .363 | −.029 |
| | OA | | | | | | | - | .023 | .202 | .569** | .290 |
| CFD velocity (m/s) | Nasal airway | | | | | | | | - | −.127 | −.246 | −.274 |
| | NA | | | | | | | | | - | .095 | .385 |
| | RA | | | | | | | | | | - | .666** |
| | OA | | | | | | | | | | | - |

Spearman's correlation coefficient, n = 20, **P < 0.01, *P < 0.05, AR = Acoustic rhinometry, CFD = computational fluid dynamics, NAR = nasal airway resistance (Pa/cm$^3$/s), MCA = minimal cross-sectional area (cm$^2$), LNV = lateral nasal volume 0-5 cm (cm$^3$), Nasal airway = The part front of the nasal cavity (Fig. 1), NA = nasopharyngeal airway, OA = oropharyngeal airway, RA = retropalatal airway

greater the nasal obstruction, the higher the pressure was. Increasing the number of cases in the future may make it possible to use quantified pressures and velocities to assess the extent of upper airway ventilation disorders.

One of the two patients in whom the obstruction site was in the RA was diagnosed with sinusitis, and the main complaint was that of nasal obstruction. However, the NAR determined using RM was in the normal range, and the nasal airway was not the obstruction site as per the results of the CFD analysis. Also, the other case in which the obstruction site was in the RA also had nasal obstruction as the chief complaint; however, the NAR was normal, and the nasal airway was not an obstruction site in CFD. Even if nasal obstruction is the main complaint, different upper airway sites may be obstructed. CFD analysis of the upper airway allows the evaluation of disorders in other parts of the airway. The nasal airway is part of the upper airway. Therefore, it is important to quantify the upper airway's ventilation status, and CFD analysis is considered the best method for this evaluation[29, 30]. In addition to the quantitative assessment of ventilation, CFD allows us to identify and visualize the upper airway obstruction sites. The nasal cycle was not considered in this study, and the diseases were not unified in this study; these issues need to be addressed in future trials. The present study was conducted in a single hospital in Japan, and future studies with a larger sample size are needed. In the future, we would also like to use CFD analysis to observe changes in the condition of patients with nasal and paranasal diseases following improvements and surgery. Also, CFD analysis can be helpful for subjects with communication difficulties, including infants. This method differs from RM and AR because the latter methods require patient communication. In the future, we plan to research these methodologies. With further advances in research, CFD analysis should become more valuable in the clinical setting.

**Acknowledgments**

We gratefully acknowledge the work of past and present members of our Division and Department of Otorhinolaryngology.

**Conflict of interest disclosure**

The authors have no conflicts of interest relevant to the content of this article.

**References**

1. Mihaescu M, Mylavarapu G, Gutmark EJ, *et al*. Large eddy simulation of the pharyngeal airflow associated with obstructive sleep apnea syndrome at pre and post-surgical treatment. *J Biomech*. 2011;**44**:2221–2228.
2. Yanagisawa-Minami A, Sugiyama T, Iwasaki T, *et al*. Primary site identification in children with obstructive sleep apnea by computational fluid dynamics analysis of the upper airway. *J Clin Sleep Med*. 2020;**3**:431–439.
3. Iwasaki T, Sato H, Suga H, *et al*. Influence of pharyngeal airway respiration pressure on class II mandibular retrusion in children: a computational fluid dynamics study of inspiration and expiration. *Orthod Craniofac Res*. 2017;**20**:95–101.
4. Shirazawa Y, Iwasaki T, Ooi K, *et al*. Relationship between pharyngeal airway depth and ventilation condition in mandibular setback surgery: a computational fluid dynamics study. *Orthod Craniofac Res*. 2020;**23**:313–322.
5. Wootton DM, Luo H, Persak SC, *et al*. Computational fluid dynamics endpoints to characterize obstructive sleep apnea syndrome in children. *J Appl Physiol (1985)*. 2014;**116**:104–112.
6. Farzal Z, Del Signore AG, Zanation AM, *et al*. A computational fluid dynamics analysis of the effects of size and shape of anterior nasal septal perforations. *Rhinology*. 2019;**57**:153–159.
7. Cannon DE, Frank DO, Kimbell JS, *et al*. Modeling nasal physiology changes due to septal perforations. *Otolaryngol Head Neck Surg*. 2013;**148**:513–518.
8. Nomura T, Ushio M, Kondo K, *et al*. Effects of nasal septum perforation repair on nasal airflow: an analysis using computational fluid dynamics on preoperative and postoperative three-dimensional models. *Auris Nasus Larynx*. 2018;**45**:1020–1026.
9. Garcia GJ, Rhee JS, Senior BA, *et al*. Septal deviation and nasal resistance: an investigation using virtual surgery and computational fluid dynamics. *Am J Rhinol Allergy*. 2010;**24**:46–53.
10. Radulesco T, Meister L, Bouchet G, *et al*. Correlations between computational fluid dynamics and clinical evaluation of nasal airway obstruction due to septal deviation: an observational study. *Clin Otolaryngol*. 2019;**44**:603–611.
11. Wakayama T, Suzuki M, Tanuma T. Effect of nasal obstruction on continuous positive airway pressure treatment: computational fluid dynamics analyses. *PLoS One*. 2016;**11**:e0150951. (accessed 2021 Feb 23) Available from: https://www.ncbi.nlm.nih.gov/pmc/articles/PMC4778797/pdf/pone.0150951.pdf
12. Andre RF, Vuyk HD, Ahmed A, *et al*. Correlation between subjective and objective evaluation of the nasal airway. A systematic review of the highest level of evidence. *Clin Otolaryngol*. 2009;**34**:518–525.
13. Kim CS, Moon BK, Jung DH, *et al*. Correlation between nasal obstruction symptoms and objective

parameters of acoustic rhinometry and rhinomanometry. *Auris Nasus Larynx*. 1998;**25**:45–48.
14. Ko JH, Kuo TB, Lee GS. Effect of postural change on nasal airway and autonomic nervous system established by rhinomanometry and heart rate variability analysis. *Am J Rhinol*. 2008;**22**:159–165.
15. Hasegawa M, Saito Y. Postural variations in nasal resistance and symptomatology in allergic rhinitis. *Acta Otolaryngol*. 1979;**88**:268–272.
16. Rundcrantz H. Postural variations of nasal patency. *Acta Otolaryngol*. 1969;**68**:435–443.
17. Naito K, Miyazaki S, Nonaka S. Rhinomanometry gaidorain. *Jpn J Rhinol.* 2001;**40**:327–331. (in Japanese).
18. Kase Y, Ohki M. Acoustic rhinometry gaidorain. *Jpan J Rhinol*. 2001;**40**:332–336. (in Japanese).
19. Iwasaki T, Takemoto Y, Inada E, *et al*. The effect of rapid maxillary expansion on pharyngeal airway pressure during inspiration evaluated using computational fluid dynamics. *Int J Pediatr Otorhinolaryngol*. 2014;**78**:1258–1264.
20. Iwasaki T, Suga H, Minami-Yanagisawa A, *et al*. Upper airway in children with unilateral cleft lip and palate evaluated with computational fluid dynamics. *Am J Orthod Dentofac Orthop*. 2019;**156**:257–265.
21. Iwasaki T, Saitoh I, Takemoto Y, *et al*. Evaluation of upper airway obstruction in class II children with fluid-mechanical simulation. *Am J Orthod Dentofac Orthop*. 2011;**139**:e135–e145.
22. Warren DW, Hairfield WM, Seaton D, *et al*. The relationship between nasal airway size and nasal-oral breathing. *Am J Orthod Dentofac Orthop*. 1988;**93**:289–293.
23. Warren DW. Nasal airway measurements. *Am J Orthod Dentofac Orthop*. 1988;**93**:443–445.
24. Georgalas C. The role of the nose in snoring and obstructive sleep apnoea: an update. *Eur Arch Otorhinolaryngol*. 2011;**268**:1365–1373.
25. Taasan V, Wynne JW, Cassisi N, *et al*. The effect of nasal packing on sleep-disordered breathing and nocturnal oxygen desaturation. *Laryngoscope*. 1981;**91**:1163–1172.
26. Olsen KD, Kern EB, Westbrook PR. Sleep and breathing disturbance secondary to nasal obstruction. *Otolaryngol Head Neck Surg*. 1981;**89**:804–810.
27. Craig TJ, Teets S, Lehman EB, *et al*. Nasal congestion secondary to allergic rhinitis as a cause of sleep disturbance and daytime fatigue and the response to topical nasal corticosteroids. *J Allergy Clin Immunol*. 1998;**101**:633–637.
28. Fitzpatrick MF, McLean H, Urton AM, *et al*. Effect of nasal or oral breathing route on upper airway resistance during sleep. *Eur Respir J*. 2003;**22**:827–832.
29. Gunatilaka CC, Schuh A, Higano NS, *et al*. The effect of airway motion and breathing phase during imaging on CFD simulations of respiratory airflow. *Comput Biol Med*. 2020;**127**:104099.
30. Cherobin GB, Voegels RL, Gebrim EMMS, *et al*. Sensitivity of nasal airflow variables computed via computational fluid dynamics to the computed tomography segmentation threshold. *PLoS One*. 2018;**13**:e0207178. (accessed 2021 Feb 23) Available from: https://www.ncbi.nlm.nih.gov/pmc/articles/PMC6239298/pdf/pone.0207178.pdf